RSC Advances

PAPER

View Article Online
View Journal | View Issue

Cite this: *RSC Adv.*, 2021, **11**, 33692

Preparation of a magnetic and recyclable superparamagnetic silica support with a boronic acid group for immobilizing Pd catalysts and its applications in Suzuki reactions†

Assefa Aschenaki, Fangfang Ren, Jia Liu, Wenqing Zheng, Qianyi Song, Wenhui Jia, James Jianmin Bao and Youxin Li *

Palladium is one of the best metal catalysts for Suzuki cross-coupling reaction to synthesize unsymmetrical biaryl compounds. However, homogeneous palladium (Pd) is limited in an industrial scale due to the high cost, separation, removal, and recovery issues. In this paper, a novel, high activity magnetic nanoparticles (Fe_3O_4@SiO_2-APBA-Pd) catalyst was prepared by a simple, cost-effective procedure. The as-prepared functional nanoparticles (Fe_3O_4@SiO_2-APBA) with boric acid group immobilized Pd through adding $Pd(OAc)_2$ to Fe_3O_4@SiO_2-APBA in absolute ethanol and maintaining for a certain time under a nitrogen atmosphere. The as-prepared catalyst was characterized by FT-IR, SEM, EDX, TEM, ICP-MS, XPS, and XRD. The results showed that the Pd (0.2–0.6 nm) was successfully anchored on the magnetic silica material with boric acid group. The amount of Pd was 0.800 mmol g^{-1}. This magnetic nanostructure (8–15 nm) is especially beneficial as a nanocatalyst because each nanoparticle can catalyze a reaction in a certain time without steric restriction, which could effectively improve the reaction efficiency. The current nanoparticles with the Pd catalyst could be used as a novel, green, and efficient heterogeneous catalyst for Suzuki reactions. This catalyst showed promising catalytic activity and excellent yields toward 14 kinds of Suzuki coupling reactions under mild reaction conditions, which was similar to homogeneous Pd and many reported heterogeneous Pd catalysts. In addition, the turnover number (TON) and turnover frequency (TOF) for the Suzuki reaction were high. TOF and TON were 9048 h^{-1} and 20 250 for the Suzuki reaction of bromobenzene and phenylboronic acid. Furthermore, the nanoparticles could be easily separated by a magnet, and could be used repeatedly seven times without any significant loss in activity.

Received 24th June 2021
Accepted 13th September 2021

DOI: 10.1039/d1ra04892a

rsc.li/rsc-advances

1. Introduction

The Suzuki–Miyaura cross-coupling reaction plays a significant industrial-scale role in the production of biaryl compounds, which are widely used for a variety of industrial applications, such as the synthesis of natural products, herbicides, pharmaceuticals, polymers, and agrochemicals.[1–3] In general, the easy availability of the starting materials (organic halides and boronic acids), high reactivity under mild reaction conditions, the tolerance to a wide range of functionalities, the formation of nontoxic products, the small amount of catalyst used in the reaction, and the possibility of using water as a solvent or co-solvent contribute to their increasing interest.[4] Homogeneous palladium (Pd) complexes have been widely explored as catalysts for this kind of reaction.[5–8] Despite the high activity and selectivity of these complexes, they have enjoyed only limited utility in industrial processes because of the challenges associated with their separation, removal, recovery, recycling, and more importantly issues with the leaching of Pd as it is an expensive metal.[9–11] To address these problems, heterogenization of the homogeneous catalyst is a promising option and is highly desirable and represents an irresistible trend in research. Conventional heterogeneous catalysts utilize palladium nanoparticles immobilized on polymeric organic[12,13] or inorganic[14,15] supports. Scientists have reported many heterogeneous palladium systems, such as polybenzimidazole-supported heterogeneous palladium, aryl couplings with heterogeneous palladium, the vinylation of iodobenzene with methyl acrylate coupling with heterogeneous palladium. Their catalytic behavior strongly depend on the status of the Pd. In particular, a heterogeneous Pd catalyst demonstrated a lower catalytic activity due to the

Tianjin Key Laboratory for Modern Drug Delivery and High-Efficiency, Collaborative Innovation Center of Chemical Science and Engineering, School of Pharmaceutical Science and Technology, Tianjin University, Room C412-8, Building 24, 92 Weijin Road, Nankai District, Tianjin 300072, China. E-mail: lyx@tju.edu.cn; Fax: +86-22-2789-2820; Tel: +86-22-2789-2820

† Electronic supplementary information (ESI) available. See DOI: 10.1039/d1ra04892a

aggregation and leaching of Pd species or particles. To assist in dispersion, the valence state, and stabilizing the supported palladium nanoparticles, the nature of catalyst supports, advanced preparation procedures, and essential functionalization are considered as appropriate.[16,17] Furthermore, nanoparticles have recently emerged as efficient alternatives for the immobilization of homogeneous catalysts.[18,19] However, in order to simplify catalyst recovery and reusability of the particles, magnetic nanoscale particles have recently emerged in catalyst science, which could be rapidly isolated from the reaction mixture using an external magnet.[20] More importantly, magnetic separation is more effective and easier than filtration or centrifugation.[21] Among the various magnetic nanoscale particles, Fe_3O_4 magnetic nanoparticles have many advantages, such as easy preparation, high surface area, and low toxicity.[22,23] Thus, they can efficiently bridge the gap between homogeneous and heterogeneous catalysis while preserving the desirable attributes of both systems.[18,19,24]

The noble Pd nanoparticles with a small size and highly uniformly dispersed on support materials are still full of challenges. For these reasons, scientists continue to search for proper ligands to improve the catalyst stability.[25] In the past decade, boronic acid (BA) ligands have emerged as popular ligands with broad interests and applications in chemistry, physics, mineralogy, biology, pharmacy, *etc.*[26–28] Aminophenylboronic acid (APBA) is the most commonly used chemical compound to introduce the BA group.[29] However, to the best of our knowledge, there is no report on preparing an immobilized Pd catalyst using boronic acids as ligands. Consequently, in this paper, we developed a novel and highly efficient way to make a recoverable Pd catalyst by using boronic acid as the capturing functional group. Meanwhile, the immobilized Pd was characterized by Fourier transform infrared spectroscopy (FT-IR), scanning electron microscopy (SEM), energy-dispersive X-ray spectroscopy (EDX), transmission electron microscopy (TEM), atomic absorption spectroscopy (AAS), inductively coupled plasma-mass spectrometry (ICP-MS), X-ray photoelectron spectroscopy (XPS), and X-ray diffraction (XRD). Its activity was evaluated by a series of Suzuki coupling reactions.

2. Experimental

2.1 Reagents and chemicals

All the chemicals were used as received without further purification. Iron chloride hexahydrate ($FeCl_3 \cdot 6H_2O$, >99%), ferrous chloride tetrahydrate ($FeCl_2 \cdot 4H_2O$, >99%), and potassium carbonate (≥99.5%) were from Tianjin Yuanli Real & Lead Co., Ltd (Tianjin, China). Also, 3-aminopropyltrimethoxysilane (APTMS) was obtained from Qufu Chenguang Chemical Co., Ltd (Shandong, China). Tetraethylorthosilicate (TEOS, ≥28.0% SiO_2) and sodium silicate ($Na_2SiO_3 \cdot 5H_2O$, 28.0–30% Na_2O) were from Tianjin Kemiou Chemical Reagent Co., Ltd (Tianjin, China), while the 3-aminophenylboronic acid monohydrate (98%) was from Shanghai Bide Pharmatech Co., Ltd (Shanghai, China). Ammonia solution (25%), sodium citrate (≥99.0%) and methanol (≥99.5%) were from Tianjin Fengchuan Chemical Reagent Technology Co., Ltd (Tianjin, China). Sodium borohydride ($NaBH_4$, ≥98.0%), sodium carbonate (≥99.8%), sodium bicarbonate (≥99.5%), ethanol (≥99.7%), and potassium monobasic phosphate (≥99.5%) were from Tianjin Jiangtian Chemical Technology Co., Ltd (Tianjin, China). Sodium hydroxide (≥96.0%) was from Tianjin Hengshan Chemical Technology Co., Ltd (Tianjin, China). Hydrochloric acid (HCl, 36.0–38.0%) was from Lianlong Bohua (Tianjin) Medicinal Chemical Co., Ltd (Tianjin, China). Toluene (≥99.5%) and acetone (≥99.0%) were from Tianjin Damao Chemical Reagent Factory (Tianjin, China). Glutaraldehyde (50%) was from Tianjin Beifang Tianyi Chemical Reagent Factory (Tianjin, China). Potassium dihydrogen phosphate (≥99.0%) was from Tianjin Guangfu Technology Development Co., Ltd (Tianjin, China). Sodium cyanoborohydride ($NaCNBH_3$, 95%) was from Tianjin Kaiyin Technology Co., Ltd (Tianjin, China). Biphenyl was from Shanghai Macklin Biochemical Co., Ltd (Shanghai, China). Bromobenzene (99%) was from Shanghai Yien Chemical Technology Co., Ltd (Shanghai, China). Palladium(II) acetate (47% Pd) and phenyl boronic acid (98%) were from Shanghai Eybridge Chemical Technology Co., Ltd (Shanghai, China). Chloroform D ($CDCl_3$, 99.8%) was from Shanghai Meryer Chemical Technology Co., Ltd (Shanghai, China). Finally, the deionized water was from Tianjin Yongyuan Distilled Water Manufacturing Center.

2.2 Instruments

The immobilized Pd catalyst and other intermediates were characterized. The functional groups in Fe_3O_4, Fe_3O_4@SiO_2, Fe_3O_4@SiO_2-AP, Fe_3O_4@SiO_2-GA, Fe_3O_4@SiO_2-APBA, and Fe_3O_4@SiO_2-APBA-Pd were identified through pressing disks containing KBr and then scanning on a TENSOR 27 Fourier transform infrared spectrometer (Bruker, Germany). A S2800 SEM (Hitachi, Japan) making use of a focused beam of high-energy electrons to generate a variety of signals at the surface of solid specimens was used to analyze the morphology of the prepared Fe_3O_4, Fe_3O_4@SiO_2, and Fe_3O_4@SiO_2-APBA-Pd. The PHI-1600 energy-dispersive X-ray spectroscopy system (PerkinElmer, USA) was used to confirm the elements (Fe, Pd, Si, C, B, and O) and their distribution on the surface of Fe_3O_4@SiO_2-APBA-Pd. A JEM-2100F TEM system (JEOL, Japan) was used for determining the Pd in Fe_3O_4@SiO_2-APBA-Pd, which was prepared by placing a drop containing particles on a coated-carbon grid. The amounts of Pd in Fe_3O_4@SiO_2-APBA-Pd and in the Suzuki reaction solution were monitored using a 180–80 atomic absorption spectrophotometer (Hitachi, Japan) and an Agilent 7700X inductively coupled plasma-mass spectrometer (Agilent, USA). The electronic state of Pd in Fe_3O_4@SiO_2-APBA-Pd was analyzed by X-ray photoelectron spectroscopy (X-Max, England). A D/MAX-2500 diffractometer (Rigaku, Japan) with Cu-Kα radiation ($\lambda = 0.1540$) was used to identify the crystal lattice structure of Fe_3O_4@SiO_2-APBA-Pd in the 2θ range of 10°–90° at a scan speed of 4° min^{-1}. All the Suzuki reactions were monitored by an LC 3000 high-performance liquid chromatography system (Chuangxintongheng, China). All the products of the Suzuki reactions were purified by a C18 solid-phase

extraction (SPE) column (Aumi, China) and identified by Icon nuclear magnetic resonance (NMR, Bruker, Germany).

2.3 Preparation of the immobilized Pd catalysts

2.3.1 Preparation of magnetic Fe_3O_4 with silica gel-coated (Fe_3O_4@SiO_2) nanoparticles. Magnetic Fe_3O_4 particles were synthesized by a chemical co-precipitation method.[30] Briefly, a mixture of $FeCl_3 \cdot 6H_2O$ (5.838 g, 0.0216 mol) and $FeCl_2 \cdot 4H_2O$ (2.147 g, 0.0108 mol) was dissolved in 100 mL deionized water at 80 °C under a N_2 atmosphere with vigorous mechanical stirring. Then, 15 mL of 25% NH_4OH was added quickly into the reaction mixture. After stirring for 30 min, the reaction mixture was cooled to room temperature, and the black precipitate (magnetic Fe_3O_4 particles) was magnetically separated and washed several times by distilled water. The obtained product was dried at 60 °C for 24 h.

The magnetite Fe_3O_4@SiO_2 particles were prepared by a two-step sol–gel approach.[31] First, the surface of Fe_3O_4 nanoparticles was coated by a silica layer. Briefly, 4.5 g of sodium silicate was dissolved in 120 mL of distilled water in a glass beaker. With mechanical stirring, the pH of the sodium silicate solution was adjusted to ~12 by sodium hydroxide. After adding 4.0 g Fe_3O_4 fine particles, the mixture was treated ultrasonically for 30 min. Then, the mixture was heated to 85 °C under a nitrogen gas atmosphere for 3 h. After the reaction, the pH of the mixture was adjusted to 6 using 2 mol L^{-1} hydrochloric acid. Then, the precipitates were washed several times using distilled water and collected by magnetic decantation. The Fe_3O_4@SiO_2 was then coated again to ensure that the desired amount of silica was on all the magnetite Fe_3O_4.[32,33] The above Fe_3O_4@SiO_2 was re-dispersed in a 100 mL methanol/water (1 : 1, v/v) mixture followed by the addition of 1 mL ammonium hydroxide (25% aqueous solution). The mixture was heated to 85 °C under stirring condition and a N_2 atmosphere. After the dropwise addition of 1 mL of TEOS in 10 mL methanol, the mixture was gently stirred for 1 h. The nanoparticles (Fe_3O_4@SiO_2) were collected by a magnet and washed several times with distilled water and ethanol. Finally, the particles were dried at 60 °C under vacuum and a brown yellow solid was obtained.

2.3.2 Preparation of the boric acid-functionalized Fe_3O_4@SiO_2 (Fe_3O_4@SiO_2-APBA). The magnetic Fe_3O_4@SiO_2 particles (5.0 g) were ultrasonically dispersed in anhydrous toluene (120 mL) for 30 min. Then, they was transferred into a 250 mL three-necked flask and heated to 110 °C. Under stirring conditions, 3-aminopropyltrimethoxysilane (7 mL) was added into this mixture. The temperature was kept at 110 °C with continuous stirring for 24 h. The particles of Fe_3O_4@SiO_2 with an aminopropyl group (Fe_3O_4@SiO_2-AP) were separated by a magnet, washed with acetone and toluene, and then dried at 60 °C for 24 h. Subsequently, 5.0 g of Fe_3O_4@SiO_2-AP particles was dispersed in 50 mL 0.1 mol L^{-1} phosphate buffered

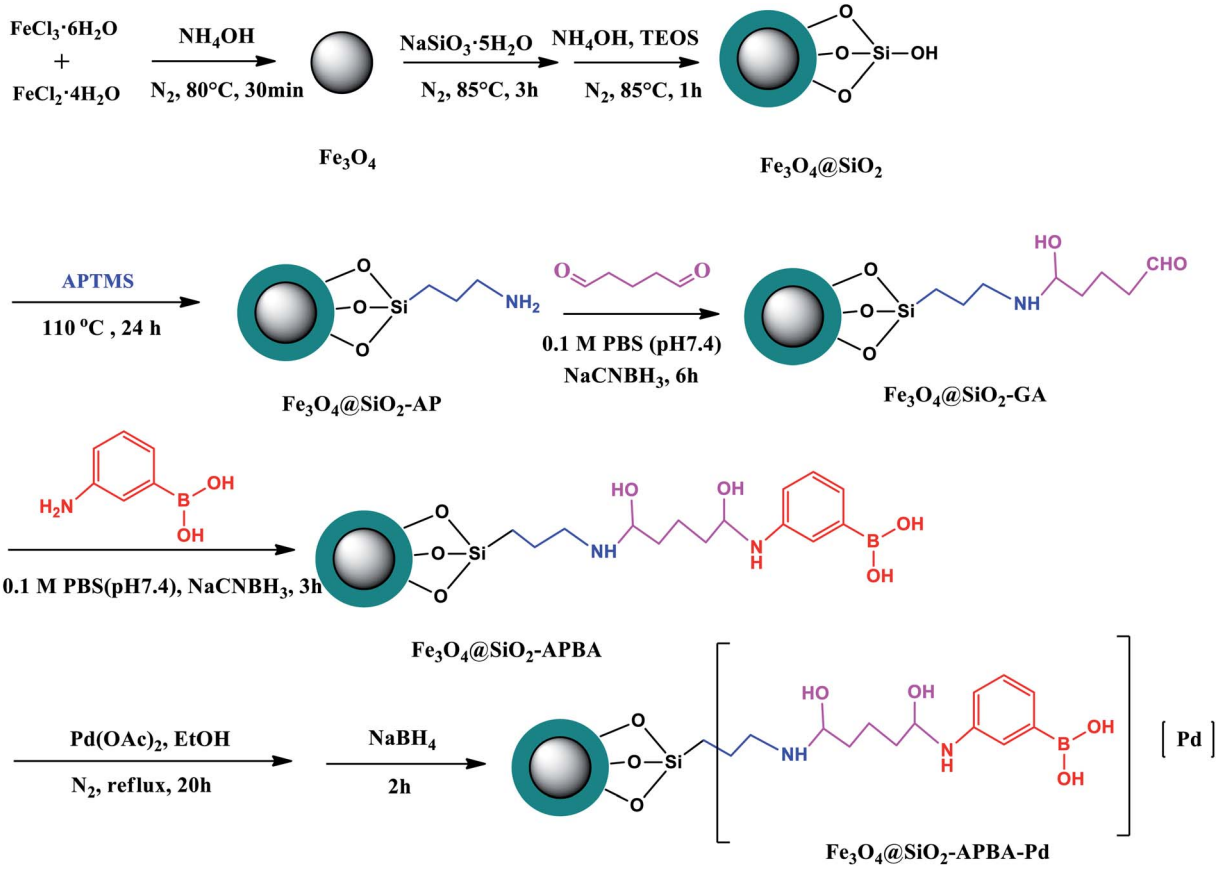

Fig. 1 Schematic diagram of the synthesis of the Fe_3O_4@SO_2-APBA-Pd catalyst.

solution (PBS, containing 10 mL 25% glutaraldehyde) at pH 7.4. To enhance the stability of the grafted glutaraldehyde, 1 mL of 0.1 mg mL^{-1} sodium cyan borohydride ($NaCNBH_3$) was added into the mixture to reduce CN to C–N and then the mixture was mechanically stirred at room temperature for 6 h. After being collected by a magnet, the Fe_3O_4@SiO_2-AP modified by glutaraldehyde (Fe_3O_4@SiO_2-GA) was washed and dried at 60 °C. Then, 2.5 g of the dry Fe_3O_4@SiO_2-GA was dispersed in 0.1 mol L^{-1} PBS solution (50 mL, pH 7.4) containing 0.5 g APBA and 0.2 g $NaCNBH_3$. The mixture was gently stirred for an extra 3 h at room temperature. Finally, the Fe_3O_4@SiO_2-APBA magnetic particles were orderly washed, collected, and dried at 80 °C for further use.

2.3.3 Preparation of the immobilized palladium catalyst (Fe_3O_4@SiO_2-APBA-Pd). The magnetic particles of Fe_3O_4@SiO_2-APBA (1.0 g) were dispersed in 20 mL absolute ethanol in an ultrasonic bath for 20 min, and then $Pd(OAc)_2$ (0.3 g) was added. The resulting mixture was refluxed for 20 h under a nitrogen atmosphere. Subsequently, an excess of 0.203 g (5.26 mmol) $NaBH_4$ was added to reduce the Pd particles, and the mixture was refluxed for an extra 2 h under a N_2 atmosphere. After that, the final product was magnetically separated and washed with copious amounts of absolute ethanol and then dried at 60 °C. A schematic diagram of the synthesis of the Fe_3O_4@SO_2-APBA-Pd catalyst is shown in Fig. 1.

2.4 General procedure for the Suzuki reaction

Unless otherwise stated, the Suzuki reactions were performed as follows: 1 mmol aryl halides in 3 mL of water/ethanol (1 : 1, v/v), 1.1 mmol phenyl boronic acid, 3 mmol K_2CO_3, and 10 mg Fe_3O_4@SiO_2-APBA-Pd catalyst (also containing 8.00×10^{-6} mol Pd) were added into a Schlenk tube and mixed. The mixture was stirred for 80 min at 60 °C. At the end of the coupling reactions, ethanol (5 mL) was added and then the catalyst was collected by an external magnet. The supernatant was transferred and fixed at 8 mL and then stored as the sample stock solution.

2.5 Analysis of the products from the Suzuki reactions by HPLC

High-performance liquid chromatography (HPLC) was used to analyze all the products of the Suzuki reactions. Unless otherwise stated, the chromatographic conditions were as follows: the column was an Aumi™ C18, 4.6 × 250 mm, 5 μm; the temperature was at room temperature; the mobile phase was a mixture of distilled water and acetonitrile (40 : 60, v/v); the flow rate was 1 mL min^{-1} and the injection volume was 10 μL; the detection wavelength was at 214 nm. Also, the samples were diluted with acetonitrile and filtered before the HPLC analysis.

3. Result and discussion

3.1 Characterization

The characterization of the Fe_3O_4@SiO_2-APBA-Pd, such as the complete composition, morphology, size, and electronic state characterization was performed by a series of techniques, including FT-IR, SEM, TEM, EDX, AAS, ICP-MS, XPS, and XRD.

FT-IR spectroscopy was used for monitoring the preparation process of Fe_3O_4@SiO_2-APBA-Pd and confirming the surface structure of the materials. The FT-IR spectra of Fe_3O_4, Fe_3O_4@SiO_2, Fe_3O_4@SiO_2-AP, Fe_3O_4@SiO_2-GA, Fe_3O_4@SiO_2-APBA, and Fe_3O_4@SiO_2-APBA-Pd are presented in Fig. 2. The two strong absorptions at 562 and 634 cm^{-1} were attributed to the Fe–O stretching vibration, which are characteristic peaks for Fe_3O_4.[31,34] Two strong absorptions were observed in each FT-IR spectrum, which indicated that Fe_3O_4 nanoparticles existed in all the intermediates and in the Fe_3O_4@SiO_2-APBA-Pd catalyst. The characteristic stretching vibration of a hydroxyl group was at 3421 cm^{-1}, which was also observed in all the materials. Meanwhile, the band centered at 1623 cm^{-1} was ascribed to the vibration of OH, which was related to the isolated hydroxyl groups on the silica surface. The strong absorption band centered at 1035 cm^{-1} was characteristic of Si–O stretching, which verified the success of the coating of SiO_2 on the surface of the Fe_3O_4 nanoparticles. In the FT-IR spectrum of Fe_3O_4@SiO_2-AP, an aminopropyl group was confirmed by the stretching vibrations of an aliphatic C–H group that appeared at 2915 and 2857 cm^{-1}. In addition, a band appeared and overlapped with the stretching vibration of an –OH group at 3421 cm^{-1}, which was also related to the stretching vibration of N–H. In the spectra of Fe_3O_4@SiO_2-APBA and Fe_3O_4@SiO_2-APBA-Pd, the appearance of peaks around 1378 and 2342 cm^{-1} corresponded to B–O and C–N stretching, respectively, which verified the existence of boric acid groups.

The morphologies of the prepared Fe_3O_4 and Fe_3O_4@SiO_2-APBA-Pd were analyzed by SEM, and the results are shown in Fig. 3. The images indicated all of these prepared materials were nanoscale particles. Moreover, due to the high-density growth, some agglomerations in the nanoparticles could also be observed (Fig. 3a), which could be dispersed well in solution. Most of the nano-level particles almost possessed a spherical

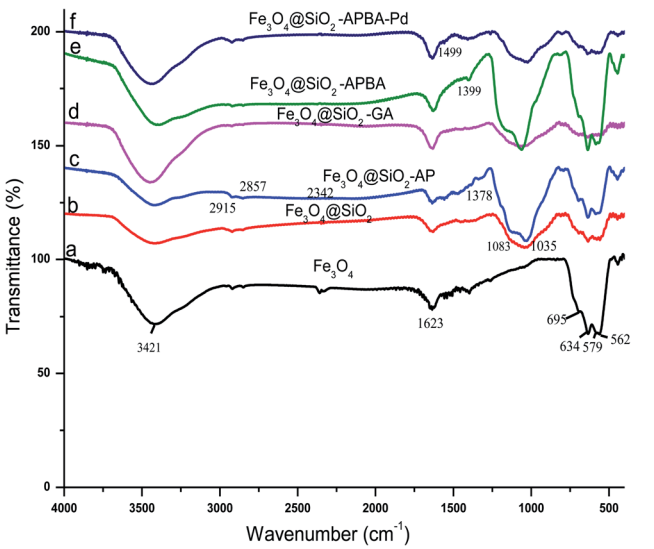

Fig. 2 FT-IR spectra of Fe_3O_4 (a), Fe_3O_4@SiO_2 (b), Fe_3O_4@SiO_2-AP (c), Fe_3O_4@SiO_2-GA (d), Fe_3O_4@SiO_2-APBA (e), and Fe_3O_4@SiO_2-APBA-Pd (f).

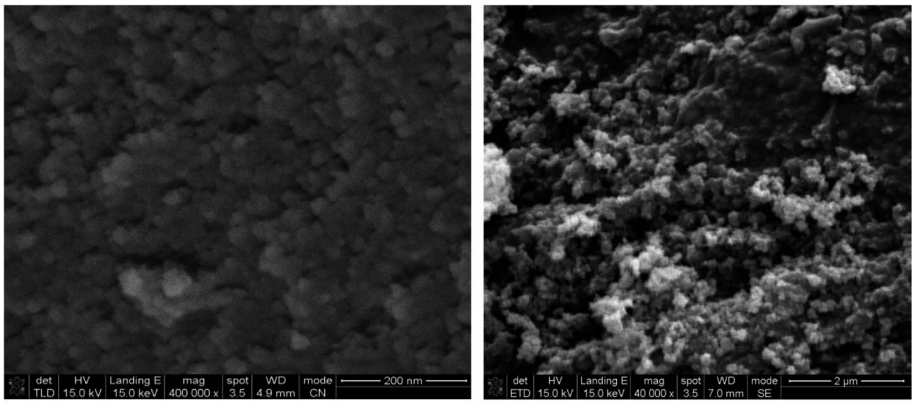

Fig. 3 SEM images of Fe_3O_4 (a) and Fe_3O_4@SiO_2-APBA-Pd (b).

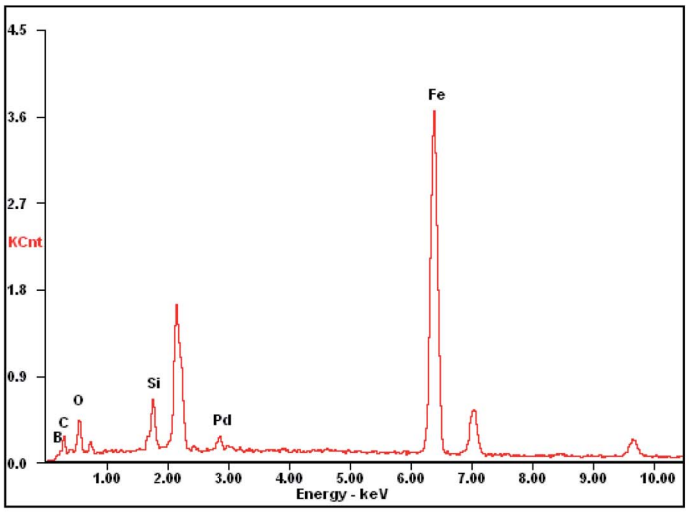

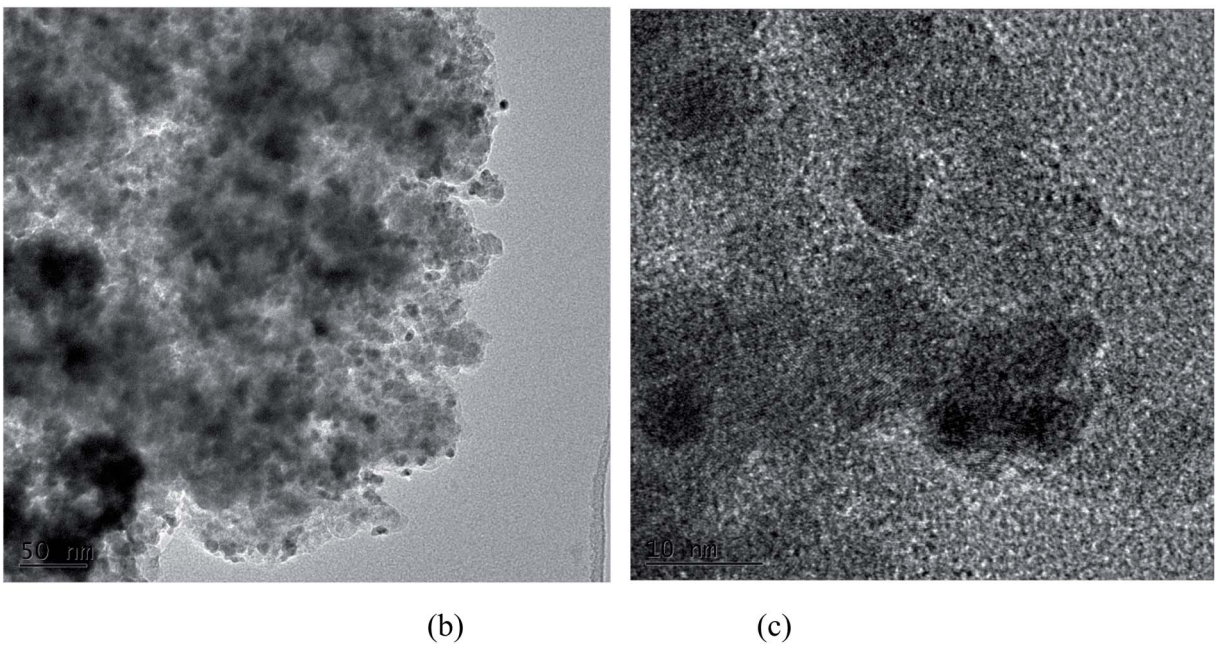

Fig. 4 EDX spectrum (a) and TEM image of Fe_3O_4@SiO_2-APBA-Pd (b) and (c).

shape; however, some elongated nanoscale particles were also seen in the SEM images.

Energy-dispersive X-ray spectroscopy (Fig. 4a) was performed for investigating the types of elements in the immobilized catalyst. The results confirmed not only the presence of palladium but also a lot of C, B, Si, O, and Fe in the Fe_3O_4@SiO_2-APBA-Pd. The presence of Si (wt%: 5.76), O (wt%: 23.41), and Fe (wt%: 36.11) signals in the EDX verified Fe_3O_4 had been coated by silica. The C (wt%: 16.88) and B (wt%: 10.25) signals indicated that the Fe_3O_4@SiO_2 was successfully modified to prepare Fe_3O_4@SiO_2-APBA. The Pd (wt%: 7.60) demonstrated that palladium was successfully immobilized on Fe_3O_4@SiO_2-APBA. The TEM image (Fig. 4b) showed that Fe_3O_4@SiO_2-APBA-Pd was in the form of nanoparticles in the size range of 8–15 nm. Moreover, the Pd had a narrow particle size of about 0.2–0.6 nm, which was dispersed uniformly on the surface of the support. This result explained that Pd was successfully anchored on the Fe_3O_4@SiO_2-APBA to form Pd heterogeneous catalysts.

The exact Pd amount in Fe_3O_4@SiO_2-APBA-Pd was firstly determined by ICP-MS. First, 40 mg Fe_3O_4@SiO_2-APBA-Pd was added into a digestion tank containing a 4 mL mixture acid of analytically pure HNO_3 and HCl (v/v, 3 : 1). After the mixture was digested for 24 h at room temperature, distilled water was added to make the total volume up to 30 mL. Then, the Pd amount was determined by a standard curve method. The data showed that the Pd amount in Fe_3O_4@SiO_2-APBA-Pd was 0.800 mmol g^{-1}, which indicated about 60.1% Pd in $Pd(Ac)_2$ was immobilized. This result was apparently higher than in the other heterogeneous Pd catalyst. Thus, we guessed that the boric acid group was beneficial for forming a chelated ring between Pd and the -$B(OH)_2$ group to anchor so much Pd catalyst.

In the XPS spectrum (Fig. 5), the peaks at binding energies of 101.2, 191.6, 285, 335.4, 399.8, 534.4, 698.7, and 1072 eV were assigned to Si, B, C, Pd, N, O, Fe, and Na, respectively. The presence of silicon and oxygen species confirmed that Fe_3O_4@SiO_2-APBA-Pd was coated over the surface of the Fe_3O_4 nanoparticles. Moreover, the characteristic doublet peaks at 335.4 and 340.6 eV, assignable to the $3d_{5/2}$ and $3d_{3/2}$ states, respectively, confirmed the zero oxidation state of palladium.[35]

The wide-angle XRD pattern was used for analyzing Fe_3O_4@SiO_2-APBA-Pd. The crystalline peaks at diffraction angles $2\theta = 30.4°$, 35.7°, 40°, 43.3°, 46.4°, 57.4°, 62.9°, 67.9°, and 81.9° represented the structure of Fe_3O_4@SiO_2-APBA-Pd. Sharp diffraction peaks were also easily noticed at $2\theta = 35.7°$ and 40°, which were characteristic of iron oxide and palladium, respectively. In addition, the XRD pattern (Fig. 6) showed the uniform distribution of palladium on the magnetic support, indicating that it had been successfully stabilized on the surface of the Fe_3O_4 particles.

The characterization results above, namely the FT-IR, SEM, EDX, TEM, AAS, ICP-MS, XPS, and XRD results, verified that the ligand of boronic acid had been successfully modified on the surface of Fe_3O_4@SiO_2 and that Pd was successfully anchored on the nanoscale magnetic Fe_3O_4@SiO_2-APBA support.

3.2 Catalytic performance of Fe_3O_4@SiO_2-APBA-Pd

3.2.1 Catalyzing the Suzuki reaction between bromobenzene and phenylboronic acid. The catalytic activity of Fe_3O_4@SiO_2-APBA-Pd was evaluated in a series of Suzuki coupling reactions. In order to evaluate the immobilized Pd under optimum conditions, the reaction between bromobenzene and phenylboronic acid was chosen as a model reaction and the reaction conditions were investigated, including the solvent, base, reaction temperature, time, and catalyst amount.

3.2.1.1 Effect of the solvent on the biphenyl yield. The solvent may affect the activity of the catalyst and the yield from the Suzuki reaction. In the literature, the solvents used for Pd-catalyzed cross-couplings of arylboronic acids were typically organic solvents or water/organic solvent mixtures. To evaluate the catalytic ability of the prepared Fe_3O_4@SiO_2-APBA-Pd, we first investigated the effect of the solvent on the biphenyl yields obtained by the Suzuki reactions. Four kinds of common solvent mixtures commonly used in Suzuki reactions were

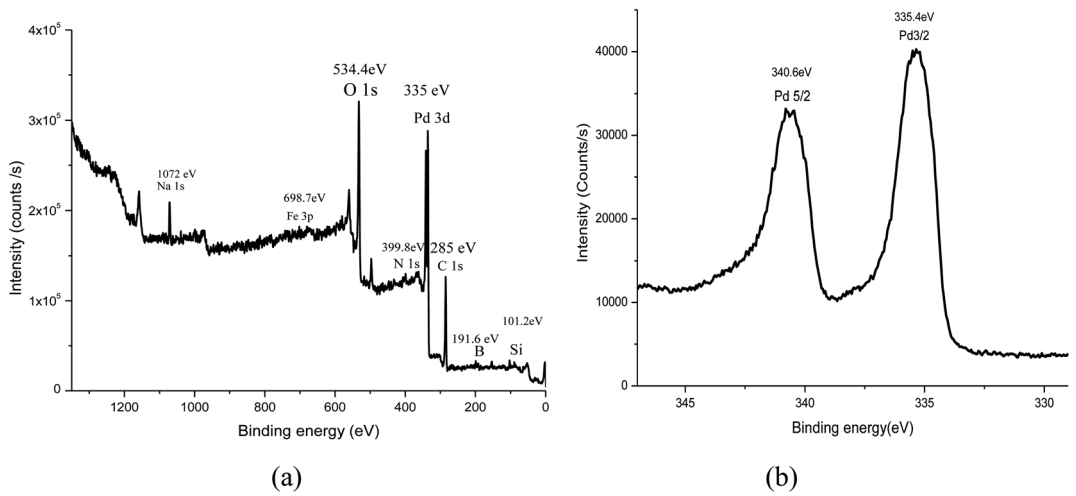

Fig. 5 XPS spectra of Fe_3O_4@SiO_2-APBA-Pd wide scan (a) and Pd 3d (b).

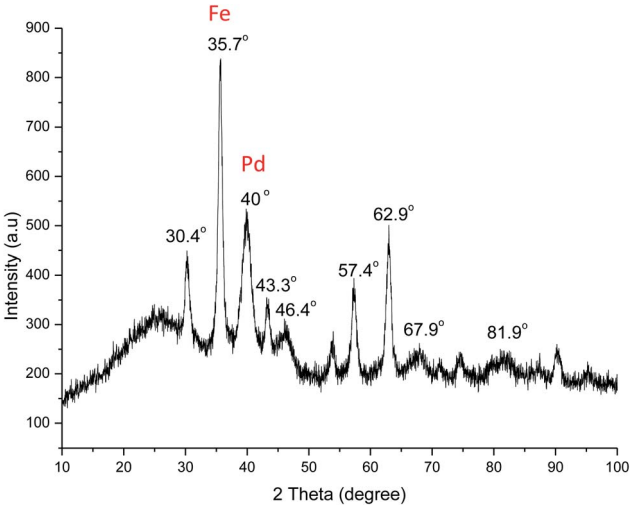

Fig. 6 XRD patterns of Fe_3O_4@SiO_2-APBA-Pd.

employed: EtOH/H_2O (v/v, 1 : 1), toluene/H_2O (v/v, 2 : 1), toluene/MeOH (v/v, 1 : 1), and MeOH/H_2O (v/v, 1 : 1). The other conditions, including 10 mg Fe_3O_4@SiO_2-APBA-Pd (containing 8.00 μmol Pd), 1.0 mmol bromobenzene, 1.1 mmol $PhB(OH)_2$, 3 mmol K_2CO_3, 3 mL solvent volume, and 80 min reaction time, were kept constant. The results are summarized in Table 1 (entries 1–4). A significant solvent effect was observed in which the nature of the solvent significantly affected the conversion of the coupling reaction. When MeOH/H_2O (v/v, 1 : 1) was used as the solvent, the biphenyl yield was only 18%. However, when the solvent was changed to toluene/MeOH (v/v, 1 : 1) and toluene/H_2O (v/v, 2 : 1), the yields increased to 48% and 65%, respectively. The best yield (88%) was obtained when EtOH : H_2O (v/v, 1 : 1) was used as the solvent. According to these results, we guessed the solvent polarity affected the whole of the Suzuki reaction. The MeOH/H_2O mixture could not effectively activate the heterogeneous Pd and dissolved the reactant and product. With the application of the EtOH/H_2O mixture with a low solvent polarity, the activation effect on the heterogeneous Pd quickly increased and the solubility of the products of the Suzuki reaction also increased. When the toluene mixture was employed, the low solvent polarity increased the solubility of the products from the Suzuki reaction but its activation effect caused the heterogeneous Pd to decrease. Thus, EtOH : H_2O (v/v, 1 : 1) was employed in the following experiments.

3.2.1.2 Effect of the base on the biphenyl yields. The base could affect the Suzuki reaction. For example, it can affect the charged state and the solubility of the reactants and products as well as causing the activity of the Pd catalyst to decrease or increase the Suzuki reaction yield. Thus, our next investigations were focused on the effect of the base on the model Suzuki reaction. Under the same conditions, six kinds of bases were investigated: $NaHCO_3$, Na_2CO_3, KOH, NaOH, K_2CO_3, and Et_3N. The results (Table 1, entries 1 and 5–11) indicated the presence of the base or the species of the base had a significant effect on the Suzuki coupling reaction. The reaction did not occur in the absence of a base (Table 1, entry 11), even when the time was extended to 720 min. Among the examined six bases, it was found that K_2CO_3 acted as an excellent base for this reaction (Table 1, entry 1). In the presence of monobasic KOH, NaOH, $NaHCO_3$, organic Et_3N, and bibasic Na_2CO_3, low yields (6.8%, 11%, 13%, 20%, and 43%) of biphenyl were observed (Table 1, entries 9, 10, 7, 8, and 6). The biggest difference between the monobasic and bibasic bases was that KOH and NaOH are stronger bases, while K_2CO_3 and Na_2CO_3 are weak bases, based on their known K_b values. As previously reported by Knecht and co-workers[36] for KOH or NaOH, the amount of free and reactive hydroxide was higher compared to with the K_2CO_3 and Na_2CO_3

Table 1 Optimization of the reaction parameters for the Suzuki reaction of bromobenzene and phenyl boronic acid[a]

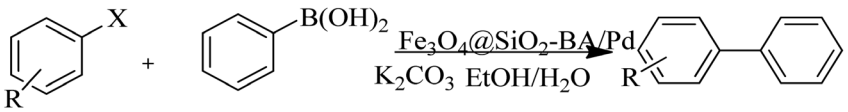

Entry	Pd (μmol)	Solvent	Base	Time (min)	Temperature (°C)	Yield (%)
1	8.00	EtOH/H_2O (1 : 1)	K_2CO_3	80	60	88
2	8.00	Toluene/H_2O (2 : 1)	K_2CO_3	80	60	65
3	8.00	Toluene/MeOH (1 : 1)	K_2CO_3	80	60	48
4	8.00	MeOH/H_2O (1 : 1)	K_2CO_3	80	60	18
5	8.00	EtOH/H_2O (1 : 1)	K_2CO_3	100	80	54
6	8.00	EtOH/H_2O (1 : 1)	Na_2CO_3	100	80	43
7	8.00	EtOH/H_2O (1 : 1)	$NaHCO_3$	100	80	20
8	8.00	EtOH/H_2O (1 : 1)	Et_3N	100	80	13
9	8.00	EtOH/H_2O (1 : 1)	NaOH	100	80	11
10	8.00	EtOH/H_2O (1 : 1)	KOH	100	80	6.8
11	8.00	EtOH/H_2O (1 : 1)	No base	720	60	Trace

[a] Reaction conditions: bromobenzene (1.0 mmol), $PhB(OH)_2$ (1.1 mmol), base (3 mmol), 10 mg Fe_3O_4@SiO_2-APBA-Pd, solvent (3 mL).

systems, which resulted in a strong combination with palladium species, leading to a decrease in the biphenyl yield. Based on these results we found that a moderate base capacity was necessary to perform the coupling reaction in the presence of the Fe_3O_4@SiO_2-APBA-Pd catalyst. Thus, K_2CO_3 was chosen for the following experiments.

3.2.1.3 Effect of temperature on the biphenyl yields. The activity of a catalyst is affected by the reaction temperature. Thus, a series of temperatures, namely 25 °C, 40 °C, 60 °C, 80 °C, and 100 °C, were investigated. According to the data, the yields of biphenyl gradually increased from 43.2% to a maximum (87.8%) with the increase in temperature to 60 °C. However, with continuously increasing the temperature, the activity of the catalyst decreased and the biphenyl yield dropped down to 40.8% under 100 °C. We deduced that the temperature affected the activity of the immobilized Pd catalyst. Thus, 60 °C was chosen for the following experiments.

3.2.1.4 Effect of the reaction time on the biphenyl yields. To explore the optimum time, different reaction times (40, 60, 80, 100, and 120 min) were investigated. The results indicated that the yield of the model Suzuki reaction gradually increased from 43.6% (40 min) to 87.8% (80 min) with longer time. However, continuously increasing the time did not lead to the yields continuing to increase. According to the data, 80 min was selected as the optimal reaction time.

3.2.1.5 Effect of the amount of Fe_3O_4@SiO_2-APBA-Pd on the biphenyl yields. As is well known, the amount of Pd catalyst will affect the speed and yield of the Suzuki reaction. Before we investigated the effect of the amount of Fe_3O_4@SiO_2-APBA-Pd, we performed the model Suzuki reaction in the absence of Fe_3O_4@SiO_2-APBA-Pd. The data showed that the yield of biphenyl was 0, even when the time was extended to 720 min. This showed that the Suzuki reaction could only be carried out under catalyst assistance. After this, we explored the effect of the amount of Fe_3O_4@SiO_2-APBA-Pd. We employed 4, 6, 8, 10, 15, 16, and 18 mg Fe_3O_4@SiO_2-APBA-Pd to perform the model Suzuki reaction, which contained 3.20, 4.80, 6.40, 8.00, 12.00, 12.80, and 14.40 μmol Pd, respectively. The results showed that the amount of Pd catalyst did indeed importantly affect the Suzuki reaction. With the increase in Fe_3O_4@SiO_2-APBA-Pd from 4 to 10 mg, a dramatic increase in yield (54.2%, 58.0%, 72.2%, and 92.1%) was observed, which indicated the importance of the Pd catalyst. When the Fe_3O_4@SiO_2-APBA-Pd amount was up to 15 mg (containing 12.00 μmol Pd), the yield (97.2%) slightly increased, but no further increase in the reaction yield was observed using even higher catalyst amounts (16 and 18 mg).

To compare the catalytic ability of Fe_3O_4@SiO_2-APBA-Pd, the same model Suzuki reaction was catalyzed by homogeneous $Pd(Ac)_2$. The best yield was 93% when $Pd(Ac)_2$ was added as 3 mg (containing 13.3 μmol Pd). This was lower than for Fe_3O_4@SiO_2-APBA-Pd. This indicated our immobilized catalyst was good.

3.2.2 Catalyzing other Suzuki reactions. To further evaluate the immobilized Pd catalyst, the scope and efficiency for Fe_3O_4@SiO_2-APBA-Pd as a catalyst were investigated through employing 13 other kinds of reactants for Suzuki reactions producing various biaryl derivatives. For example, various aryl halides were employed, including I and Br. Also, both electron-donating and electron-withdrawing substituents, such as Me, OMe, CN, NO_4, CHO, and COMe substituents, were examined. All the products were qualitatively analyzed by HPLC and

Table 2 Suzuki reactions of $C_6H_5B(OH)_2$ with 14 kinds of aryl halides catalyzed by Fe_3O_4@SiO_2-APBA-Pd[a]

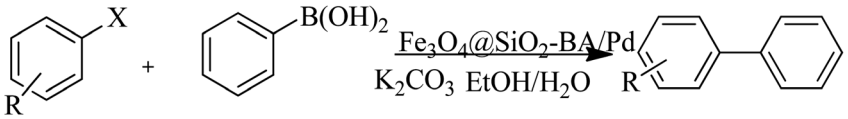

Entry	R	X	Temperature (°C)	Time (min)	Yield (%)	TOF (h^{-1})
1	H	I	60	80	94.1	9048
2	H	Br	60	80	97.2[b]	6230
3	4-Me	Br	60	80	91.4	8788
4	4-CHO	Br	60	80	90.7	8721
5	2-OMe	Br	70	120	96.7	6043
6	4-NC	Br	70	120	94.6	5912
7	4-COOH	Br	60	120	28.3	1768
8	4-$COCH_3$	Br	60	180	63.6	2650
9	4-NH_2	Br	60	80	85.4	8211
10	3-CHO	Br	60	80	87.5	8413
11	2-NO_2	Br	60	240	72.0	2250
12	4-NO_2	Br	60	240	86.7	2709
13	4-$CH_3CH_2CH_2$	Br	80	80	80.1	7701
14	C_4H_4	Br	80	240	67.5	2109

[a] Reaction conditions: benzene derivative (1 mmol), $PhB(OH)_2$ (1.1 mmol), K_2CO_3 (3 mmol), 10 mg Fe_3O_4@SiO_2-APBA-Pd, solvent (3 mL). [b] 15 mg Fe_3O_4@SiO_2-APBA-Pd.

Table 3 Suzuki reactions catalyzed by $Pd(Ac)_2$[a]

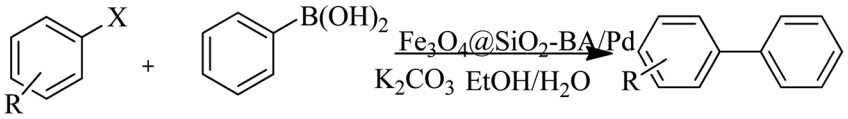

Entry	R	X	Temperature (°C)	Homogeneous yield (%)
1	H	I	60	94.4
2	H	Br	60	93
3	4-Me	Br	60	92.2
4	4-CHO	Br	60	92.9
5	2-OMe	Br	70	97.8
6	4-NC	Br	70	96.9
7	4-COOH	Br	60	30.7
8	$4\text{-}COCH_3$	Br	60	58.4
9	$4\text{-}NH_2$	Br	60	86.8
10	3-CHO	Br	60	91.2
11	$2\text{-}NO_2$	Br	60	73.8
12	$4\text{-}NO_2$	Br	60	89.2
13	$4\text{-}CH_3CH_2CH_2$	Br	80	89.7
14	C_4H_4	Br	80	68.2

[a] Reaction conditions: benzene derivative (1 mmol), $PhB(OH)_2$ (1.1 mmol), K_2CO_3 (3 mmol), 3 mg $Pd(Ac)_2$, solvent (3 mL).

compared with the standard substance. In addition, each product was purified by a solid-phase extraction (SPE) column and characterized by NMR (see ESI†). The results of the Suzuki reactions are summarized in Table 2. The results indicated that the Suzuki coupling reactions depended on the type of halide element, the positions of the substitution groups on the aromatic ring, and the effect of the various electron-donating and electron-withdrawing groups. For example, for the aldehyde-substituted aryl bromides, the position of the aldehyde group had a significant impact on the yield of the corresponding biaryl products. The highest yield was obtained when the aldehyde group was at the *para* position (90.7%) compared to at the *meta* position (87.5%). As listed in Table 2, when the coupling of aryl bromides with aryl boronic acids proceeded at 60 °C for 80 min, the corresponding products were obtained in high yields. The reaction of 2-methoxybromobenzene with phenylboronic acid showed an excellent yield (96.7%). In electron-rich or deactivated *p*-bromotoluene, the yields were high in all cases (91.4%). The electronically neutral bromobenzene produced a good amount of the desired product when coupled with arylboronic acid. Aryl iodides with arylboronic acids for the Suzuki reaction gave high yields of the corresponding products. Among Suzuki coupling reactions, some of the reactions could obtain satisfactory yields by increasing the reaction temperature and time (Table 3, entries 5, 6, and 13–14). However, for 4-bromobenzoic acid and 4-bromoacetophenone, lower yields were achieved at the given reaction condition compared with the other substrates (Table 3, entries 7 and 8), even under a prolonged the reaction time and when increasing the temperature. Among the main reasons for the low yield in the two substrates may be due to the solvent viscosity and mass transfer properties, which could affect the reaction rate and the

Table 4 Comparison of the catalytic activity of Fe_3O_4–SiO_2–APBA–Pd with other catalysts for the Suzuki cross-coupling reaction of bromobenzene and phenylboronic acid

Entry	Catalyst	Catalyst (mol%)	Condition	Time (h)	Yield (%)	Ref.
1	$Fe_3O_4/SiO_2\text{-}NH_2$/PC-Pd (NPs)	0.35	65 °C, $MeOH/H_2O$, K_2CO_3	0.75	87	37
2	GO/NHC–Pd	1	$Na_3PO_4 \cdot 12H_2O$, H_2O, 100 °C	6	91.6	38
3	CA/Pd(0)	0.5	K_2CO_3, 100 °C, H_2O	2	99	39
4	GO-CPTMS@Pd-TKHPP	10	Air EtOH : H_2O, K_2CO_3, 80 °C	0.25	99	40
5	Pd-MPA@MCM-41	1.7	PEG, 100 °C, K_2CO_3	2	94	41
6	Xerogel g1-MNPs	1	MeOH, 60 °C, Na_2CO_3	5	89	42
7	Fe_3O_4-[$Pd(TPP_)_2(OAc)_2$]	1.5	MUA-Pd, DMF, NaOH, 90 °C	12	84	43
8	Co@C@Pd	0.5	THF–H_2O (1 : 2), Na_2CO_3, 65 °C	12	92	44
9	Pd-MTAMT	0.3	DMF–H_2O (1 : 5), NaOH, 85 °C	10	85	45
10	CNT@PCOOH@Pd	0.1	DMF, K_2CO_3, 100 °C	2	77	46
11	$Fe_3O_4@SiO_2$-APBA-Pd	1.2	K_2CO_3, H_2O : EtOH, 60 °C	1.3	97.2	Present work

selectivity of catalyzed reactions due to their effect on the rate of the mass transfer of the substrates. In addition, the turnover frequency (TOF) for the 14 kinds of Suzuki reactions were monitored (Table 2, last column) to evaluate the catalytic performance of Fe_3O_4@SiO_2-APBA-Pd. High TOFs were observed. For example, the TOF for the Suzuki reaction between bromobenzene and phenylboronic acid was up to 9048 h^{-1}. In the research into palladium catalysts, the turnover number (TON) of Pd is often used as a criterion to judge performance. To calculate the TON, we employed 500 mmol bromobenzene and 550 mmol phenylboronic acid under 10 mg Fe_3O_4@SiO_2-APBA-Pd (containing 8.00 μmol Pd) to perform the Suzuki reaction. The TON was up to 20 250. The high TOF and TON indicated the immobilized Fe_3O_4@SiO_2-APBA-Pd was an excellent catalyst.

To show the catalytic ability of Fe_3O_4@SiO_2-APBA-Pd, the same Suzuki reactions catalyzed by $Pd(Ac)_2$ catalyst (3 mg, 13.3 μmol) were performed. The results are summarized in Table 3. The data indicated that the prepared Fe_3O_4@SiO_2-APBA-Pd had a similar catalytic ability to that of homogeneous $Pd(Ac)_2$.

To show the efficiency and the reactivity, the Fe_3O_4@SiO_2-APBA-Pd catalyst was compared to some of those reported using Pd-based nanoparticle catalysts. The comparison results are presented in Table 4. From the results, we can observed that our Fe_3O_4@SiO_2-APBA-Pd was superior to some results from the literature in terms of the reaction conditions, reaction time, and yields. Fe_3O_4@SiO_2-APBA-Pd was also better in terms of its easy separation compared to in the previously reported works. In addition, we observed some other advantages of Fe_3O_4@SiO_2-APBA-Pd, such as a low reaction time, it reacting at low temperature, and the use of water as a co-solvent.

3.3 Recyclability of the catalyst

The recycling of heterogeneous catalysts is an important advantage for a wide spectrum of applications. To investigate this issue, the recovery and reusability of the catalyst were examined for the Suzuki reactions of bromobenzene and phenyl boronic acid as model reactions under optimized conditions.

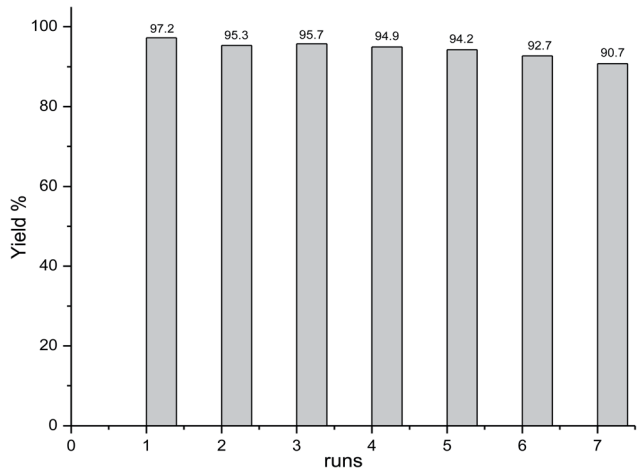

Fig. 7 Biphenyl yields with recycling Fe_3O_4@SiO_2-APBA-Pd as the catalyst.

After the completion of the first reaction, the magnetic Pd catalyst was retained in the test tube by using the external magnet and the supernatant was analyzed. Subsequently, new substrates were added to the recycled catalyst and then the next Suzuki reaction was performed. Over seven runs, the yields of biphenyl remained very high (Fig. 7). The results showed that the recycled catalysts showed a similar catalytic ability compared to the fresh ones (biphenyl yield, 97.2%). The catalytic activities of cycles 2 to 6 were 95.3%, 95.7%, 94.9%, 92.7%, and 90.7%, respectively. The catalyst was reusable and could be recycled seven times without any significant loss in activity. This indicated the immobilized Pd was very stable. The slight drop in biphenyl yield may be due to the loss of immobilized Pd, which had to be put into a round centrifuge tube, thus increasing the difficulty of completing the recycling using an external magnet. To verify this, the immobilized catalyst was collected, dried, and weighed after the 7th run. Only 8 mg was recollected, which indicated there was a half loss during 7 runs. In addition, the Pd in the supernatants was also monitored. The results showed there was only 0.0048 μmol in the supernatant of each run. Thus, we deduced that the gradually decreasing yields were due to the loss of an amount of the immobilized Pd nanocatalyst rather than the deciduous Pd. This issue could be avoided after expanding the reaction system or using a Florence flask to perform the recycling procedure. The above results indicated our Fe_3O_4@SiO_2-APBA-Pd was active, effective, and recyclable.

4. Conclusions

In this study, a novel nano-level Fe_3O_4-supported complex (Fe_3O_4@SiO_2-APBA-Pd) based on a boronic acid ligand was successfully prepared and characterized by FT-IR, SEM, TEM, EDX, AAS, ICP-MS, XPS, and XRD. The Fe_3O_4@SiO_2-APBA-Pd was sized 8–15 nm and contained 0.800 mmol g^{-1} of Pd at a narrow particle size of about 0.2–0.6 nm. The Fe_3O_4@SiO_2-APBA-Pd catalyst showed high activities in the Suzuki–Miyaura cross-coupling of 14 kinds of different aryl halides, including iodide or bromides, with phenylboronic acid under green and aerobic conditions. The Fe_3O_4@SiO_2-APBA-Pd catalyst has the advantages of being heterogeneous (*e.g.*, low cost, air-stability, easy separation, and good reusability). More importantly, the reusability experiments revealed that the Fe_3O_4@SiO_2-APBA-Pd catalyst was durable and could maintain almost the same inherent activity after seven catalytic cycles.

Conflicts of interest

There are no conflicts to declare.

Acknowledgements

The authors gratefully acknowledge the financial supports from Independent innovation foundation of Tianjin University (no. 2021XZY-0067).

References

1 R. Sedghi, B. Heidari, H. Shahmohamadi, P. Zarshenas and R. S. Varma, *Molecules*, 2019, **24**, 3048.
2 J. Magano and J. R. Dunetz, *Chem. Rev.*, 2011, **111**, 2177–2250.
3 S. E. Hooshmand, B. Heidari, R. Sedghi and R. S. Varma, *Green Chem.*, 2019, **21**, 381–405.
4 F. Alonso, I. P. Beletskaya and M. Yus, *Tetrahedron*, 2008, **64**, 3047–3101.
5 M. Adib, R. karimi-Nami and H. Veisi, *New J. Chem.*, 2016, **40**, 4945–4951.
6 R. Martin and S. L. Buchwald, *Acc. Chem. Res.*, 2008, **41**, 1461–1473.
7 J. Yin, M. P. Rainka, X. X. Zhang and S. L. Buchwald, *J. Am. Chem. Soc.*, 2002, **124**, 1162–1163.
8 O. Navarro, R. A. Kelly and S. P. Nolan, *J. Am. Chem. Soc.*, 2003, **125**, 16194–16195.
9 R. A. Sheldon, *Green Chem.*, 2007, **9**, 1273–1283.
10 P. Nehra, B. Khungar, K. Pericherla, S. Sivasubramanian and A. Kumar, *Green Chem.*, 2014, **16**, 4266–4271.
11 A. N. Marziale, D. Jantke, S. H. Faul, T. Reiner, E. Herdetweck and J. Eppinger, *Green Chem.*, 2011, **13**, 169–177.
12 S. Lebaschi, M. Hekmati and H. Veisi, *J. Colloid Interface Sci.*, 2017, **485**, 223–231.
13 M. Bakherad, A. Keivanloo, B. Bahramian and S. Jajarmi, *J. Organomet. Chem.*, 2013, **724**, 206–212.
14 A. Corma, H. Garcia and A. Leyva, *J. Mol. Catal. A: Chem.*, 2005, **230**, 97–105.
15 M. Gruttadauria, L. F. Liotta, A. M. P. Salvo, F. Giacalone, V. La Parola, C. Aprile and R. Noto, *Adv. Synth. Catal.*, 2011, **353**, 2119–2130.
16 P. Y. Wang, Z. Y. Wang, J. G. Li and Y. X. Bai, *Microporous Mesoporous Mater.*, 2008, **116**, 400–405.
17 C. Y. Ma, B. J. Dou, J. J. Li, J. Cheng, Q. Hu, Z. P. Hao and S. Z. Qiao, *Appl. Catal., B*, 2009, **92**, 202–208.
18 V. Polshettiwar and R. S. Varma, *Green Chem.*, 2010, **12**, 743–754.
19 M. Hajjami and B. Tahmasbi, *RSC Adv.*, 2015, **5**, 59194–59203.
20 S. Shylesh, V. Schunemann and W. R. Thiel, *Angew. Chem., Int. Ed.*, 2010, **49**, 3428–3459.
21 A. Ghorbani-Choghamarani, Z. Darvishnejad and B. Tahmasbi, *Inorg. Chim. Acta*, 2015, **435**, 223–231.
22 V. Polshettiwar, R. Luque, A. Fihri, H. B. Zhu, M. Bouhrara and J. M. Basset, *Chem. Rev.*, 2011, **111**, 3036–3075.
23 A. Rostami, B. Tahmasbi and A. Yari, *Bull. Korean Chem. Soc.*, 2013, **34**, 1521–1524.
24 J. Govan and Y. K. Gun'ko, *Nanomaterials*, 2014, **4**, 222–241.
25 M. Dhiman, B. Chalke and V. Polshettiwar, *ACS Sustainable Chem. Eng.*, 2015, **3**, 3224–3230.
26 L. M. Li, Y. X. Li, H. T. Wang, S. J. Liu and J. J. Bao, *Colloids Surf., A*, 2019, **570**, 322–330.
27 E. Dimitrijević and M. S. Taylor, *ACS Catal.*, 2013, **3**, 945–962.
28 L. B. Ren, Z. Liu, M. M. Dong, M. L. Ye and H. F. Zou, *J. Chromatogr. A*, 2009, **1216**, 4768–4774.
29 X. Zou, D. Liu, L. Zhong, B. Yang, Y. Lou and Y. Yin, *Carbohydr. Polym.*, 2012, **90**, 799–804.
30 S. Kumar, *J. Nanomed. Nanotechnol.*, 2013, **4**, e130.
31 L. M. Li, Y. X. Li, J. C. Yan, H. Cao, D. Y. Shao and J. J. Bao, *RSC Adv.*, 2019, **9**, 12696–12709.
32 Q. Yuan, N. Li, Y. Chi, W. Geng, W. Yan, Y. Zhao, X. Li and B. Dong, *J. Hazard. Mater.*, 2013, **254–255**, 157–165.
33 X. T. Sun, Q. Li, L. R. Yang and H. Z. Liu, *Particuology*, 2016, **26**, 79–86.
34 S. W. Hwang, A. Umar, G. N. Dar, S. H. Kim and R. I. Badran, *Sens. Lett.*, 2014, **12**, 1–5.
35 Anuradha, S. Kumari, S. Layek and D. D. Pathak, *New J. Chem.*, 2017, **41**, 5595–5604.
36 B. D. Briggs, R. T. Pekarek and M. R. Knecht, *J. Phys. Chem. C*, 2014, **118**(32), 18543–18553.
37 O. Khojasteh, V. Mirkhani and M. Moghadam, *J. Iran. Chem. Soc.*, 2017, **14**, 1139–1150.
38 S. Kim, H. J. Cho, D. S. Shin and S. M. Lee, *Tetrahedron Lett.*, 2017, **58**, 2421–2425.
39 V. W. Faria, D. G. Oliveira, M. H. Kurz, F. F. Gonçalves, C. W. Scheeren and G. R. Rosa, *RSC Adv.*, 2014, **4**, 13446–13452.
40 K. Bahrami and S. N. Kamrani, *Appl. Organomet. Chem.*, 2018, **32**, e4102–4111.
41 M. Nikoorazm, A. Ghorbani-Choghamarani, N. Noori and B. Tahmasbi, *Appl. Organomet. Chem.*, 2016, **30**, 843–851.
42 Y. T. Liao, L. S. He, J. Huang, J. Y. Zhang, L. Zhuang, H. Shen and C. Y. Su, *ACS Appl. Mater. Interfaces*, 2010, **2**, 2333–2338.
43 Z. H. Guan, J. L. Hu, Y. L. Gu, H. J. Zhang, G. X. Li and T. Li, *Green Chem.*, 2012, **14**, 1964–1970.
44 A. Schatz, T. R. Long, R. N. Grass, W. J. Stark, P. R. Hanson and O. Reiser, *Adv. Funct. Mater.*, 2010, **20**, 4323–4328.
45 A. Modak, J. Mondal, M. Sasidharan and A. Bhaumik, *Green Chem.*, 2011, **13**, 1317–1331.
46 S. M. Chergui, A. Ledebt, F. Mammeri, F. Herbst, B. Carbonnier, H. Ben Romdhane, M. Delamar and M. M. Chehimi, *Langmuir*, 2010, **26**, 16115–16121.